NASA/TM—2007-214972 ISABE–2007–1260

The Attenuation of a Detonation Wave by an Aircraft Engine Axial Turbine Stage

Dale Van Zante and Edmane Envia
Glenn Research Center, Cleveland, Ohio

Mark G. Turner
University of Cincinnati, Cincinnati, Ohio

September 2007

NASA STI Program . . . in Profile

Since its founding, NASA has been dedicated to the advancement of aeronautics and space science. The NASA Scientific and Technical Information (STI) program plays a key part in helping NASA maintain this important role.

The NASA STI Program operates under the auspices of the Agency Chief Information Officer. It collects, organizes, provides for archiving, and disseminates NASA's STI. The NASA STI program provides access to the NASA Aeronautics and Space Database and its public interface, the NASA Technical Reports Server, thus providing one of the largest collections of aeronautical and space science STI in the world. Results are published in both non-NASA channels and by NASA in the NASA STI Report Series, which includes the following report types:

- TECHNICAL PUBLICATION. Reports of completed research or a major significant phase of research that present the results of NASA programs and include extensive data or theoretical analysis. Includes compilations of significant scientific and technical data and information deemed to be of continuing reference value. NASA counterpart of peer-reviewed formal professional papers but has less stringent limitations on manuscript length and extent of graphic presentations.

- TECHNICAL MEMORANDUM. Scientific and technical findings that are preliminary or of specialized interest, e.g., quick release reports, working papers, and bibliographies that contain minimal annotation. Does not contain extensive analysis.

- CONTRACTOR REPORT. Scientific and technical findings by NASA-sponsored contractors and grantees.

- CONFERENCE PUBLICATION. Collected papers from scientific and technical conferences, symposia, seminars, or other meetings sponsored or cosponsored by NASA.

- SPECIAL PUBLICATION. Scientific, technical, or historical information from NASA programs, projects, and missions, often concerned with subjects having substantial public interest.

- TECHNICAL TRANSLATION. English-language translations of foreign scientific and technical material pertinent to NASA's mission.

Specialized services also include creating custom thesauri, building customized databases, organizing and publishing research results.

For more information about the NASA STI program, see the following:

- Access the NASA STI program home page at *http://www.sti.nasa.gov*

- E-mail your question via the Internet to *help@sti.nasa.gov*

- Fax your question to the NASA STI Help Desk at 301–621–0134

- Telephone the NASA STI Help Desk at 301–621–0390

- Write to:
  NASA Center for AeroSpace Information (CASI)
  7115 Standard Drive
  Hanover, MD 21076–1320

NASA/TM—2007-214972 ISABE–2007–1260

The Attenuation of a Detonation Wave by an Aircraft Engine Axial Turbine Stage

Dale Van Zante and Edmane Envia
Glenn Research Center, Cleveland, Ohio

Mark G. Turner
University of Cincinnati, Cincinnati, Ohio

Prepared for the
18th ISABE Conference (ISABE 2007)
sponsored by the International Society for Airbreathing Engines
Beijing, China, September 2–7, 2007

National Aeronautics and
Space Administration

Glenn Research Center
Cleveland, Ohio 44135

September 2007

Acknowledgments

This work was supported by the NASA Constant Volume Combustion Cycle Engine Technology Project, Leo Burkardt, project manager.

This work was sponsored by the Fundamental Aeronautics Program at the NASA Glenn Research Center.

Level of Review: This material has been technically reviewed by technical management.

Available from

NASA Center for Aerospace Information
7115 Standard Drive
Hanover, MD 21076–1320

National Technical Information Service
5285 Port Royal Road
Springfield, VA 22161

Available electronically at http://gltrs.grc.nasa.gov

The Attenuation of a Detonation Wave by an Aircraft Engine Axial Turbine Stage

Dale Van Zante and Edmane Envia
National Aeronautics and Space Administration
Glenn Research Center
Cleveland, Ohio 44135

Mark G. Turner
University of Cincinnati
Cincinnati, Ohio 45221

Abstract

A Constant Volume Combustion Cycle Engine concept consisting of a Pulse Detonation Combustor (PDC) followed by a conventional axial turbine was simulated numerically to determine the attenuation and reflection of a notional PDC pulse by the turbine. The multi-stage, time-accurate, turbomachinery solver TURBO was used to perform the calculation. The solution domain consisted of one notional detonation tube coupled to 5 vane passages and 8 rotor passages representing $1/8^{th}$ of the annulus. The detonation tube was implemented as an initial value problem with the thermodynamic state of the tube contents, when the detonation wave is about to exit, provided by a 1D code. Pressure time history data from the numerical simulation was compared to experimental data from a similar configuration to verify that the simulation is giving reasonable results. Analysis of the pressure data showed a spectrally averaged attenuation of about 15 dB across the turbine stage. An evaluation of turbine performance is also presented.

Introduction

It is increasingly difficult to achieve reductions in specific fuel consumption (SFC) within the current architecture of turbofan engines. One possible method to lower SFC is to fundamentally change the combustion process from deflagration to detonative combustion. In a detonation the combustion occurs coupled to a shock wave (this is the definition of a detonation wave). Because the combustion occurs at elevated pressure and temperature conditions behind the shock, it generates less entropy. This would theoretically lead to a combustor with a pressure rise and lower entropy production.

A hybrid engine configuration has been proposed where the conventional combustor is replaced by detonation tubes. However the flow presented to the turbine from the detonation tubes is highly unsteady in time, contains a strong shock wave, and is spatially non-uniform to a much greater extent than a conventional combustor exit. At least two concerns arise from the non-standard flow into the turbine: (1) How much of the detonation wave pressure pulse would survive to the engine nozzle and possibly exit as noise? (2) Can a conventional axial-flow aircraft engine turbine operate efficiently with the non-uniform inlet flow?

There is a small body of previous work on detonation tube/turbine interaction. The Air Force Research Laboratory has coupled a single detonation tube to the centrifugal turbine of an automotive turbocharger (ref. 1). The turbine produced power and survived the relatively short test with no visible damage. The turbine was operated over a wide range of conditions and its performance inferred from compressor flow measurements. Analysis of the measured pressure pulse before and after the turbine showed attenuation of 5 dB conservatively (ref. 2). A series of experiments were performed for the General Electric Turbine Interaction Program (TIP) (ref. 3). The TIP rig consisted of an eight tube pulse detonation combustor coupled to a single stage, axial turbine from a locomotive turbocharger. An extensive data set was acquired which included several tube firing sequence configurations, multiple unsteady pressure measurements throughout the flowpath, and turbine work output measurements. The turbine power was again inferred from compressor flow measurements. *Peak* pressure reductions of 9 to 10 dB were achieved. In another experiment, a six tube pulse detonation combustor was coupled to the power turbine from an auxiliary power unit (ref. 4). Peak detonation wave pressure attenuation was measured for various fill fractions, equivalence ratios, and turbine speeds. *Peak* pressure attenuation of ~15 dB was achieved for all operating speeds. For further overview of PDE development for propulsion applications see Dean (ref. 5).

The approach for the current work is to use the TURBO solver to numerically simulate a notional pulse detonation tube coupled to an aircraft engine axial turbine stage. Data from the simulation are used to determine the attenuation of the pressure wave by the turbine stage.. Details of the problem setup are given next followed by a discussion of the pressure wave character, attenuation and turbine performance.

Simulation Setup

The TURBO code is a 3D, viscous, time-accurate code which solves the Reynolds-averaged Navier-Stokes equations in a rotating Cartesian coordinate system. The equations are

spatially discretized using a modified upwind scheme (Whitfield, et al. (ref. 6)) based on Roe (ref. 7) and Osher and Chakravarthy (ref. 8). Temporal discretization is second-order accurate backward differencing. The governing equations are time-marched with an implicit scheme based on an iterative Newton algorithm with flux Jacobians computed using the flux-vector splitting technique of Steger and Warming (ref. 9) and analytical viscous Jacobians. Matrix inversion is accomplished using a symmetric Gauss-Siedel technique and multiple Newton subiterations are performed at each time step to minimize linearization error. The effects of turbulence are incorporated using a NASA/CMOTT κ-ε turbulence model (Zhu and Shi (ref. 10)) with wall functions. TURBO computes the flowfields of single or multiple blade passages within either a complete blade row or a periodic circumferential sector of a blade row, and it is capable of simulating unsteady interaction between multiple blade rows using a dynamic sliding interface. Further information on the numerical aspects of TURBO can be found in Chen and Briley (ref. 11). The GUMBO pre-processor (ref. 12) was used to set boundary conditions and prepare the necessary input files for TURBO.

Use of the TURBO code allowed the turbomachinery to be coupled with a notional detonation tube in a single simulation. The geometry simulated is the first stage high pressure turbine from a contemporary, high bypass ratio, turbofan engine. Analysis of the base configuration was presented by List et al. (ref. 13). An overview of the geometry is shown in figure 1. Two modifications of the geometry were done to make the simulation more typical of the hybrid engine configuration and to reduce the necessary computational resources. First, in a conventional engine the combustor flow is very low speed, Mach ~0.05. This is unrealistically low for the hybrid engine because the detonation tube purge time would be excessive. To raise the Mach number to ~0.2 the vane inlet region hub radius was increased (flow area decreased). The vane geometry was then extended upstream at constant area to produce a volume in which the detonation tube could be modeled. Second, the rotor blade count was changed from 68 to 64. The rotor blade geometry was not altered but the flow path area was scaled to account for the change in metal blockage. The vane count is 40, thus a periodic sector consisting of 5 vanes and 8 rotors, $1/8^{th}$ annulus, could be simulated.

The vane has 101 nodes on the chord, 55 nodes hub to case, and 45 nodes blade to blade. The rotor has 105 nodes on the chord with identical spanwise and tangential node counts as the vane. The rotor had 4 equal size cells in the tip clearance gap in the radial direction. The clearance gap is modeled as a periodic condition across the blade tip. The detonation tube volume is modeled by ~1M nodes (200x55x90) with uniform cell size in the axial and tangential directions (no stretching). The exit of the detonation tube is one vane axial chord upstream of the vane leading edge. With upstream and downstream extensions, one vane mesh is 915,750 nodes and one rotor mesh is 398,475 nodes which yields a total node count for the periodic sector of 7.77M nodes.

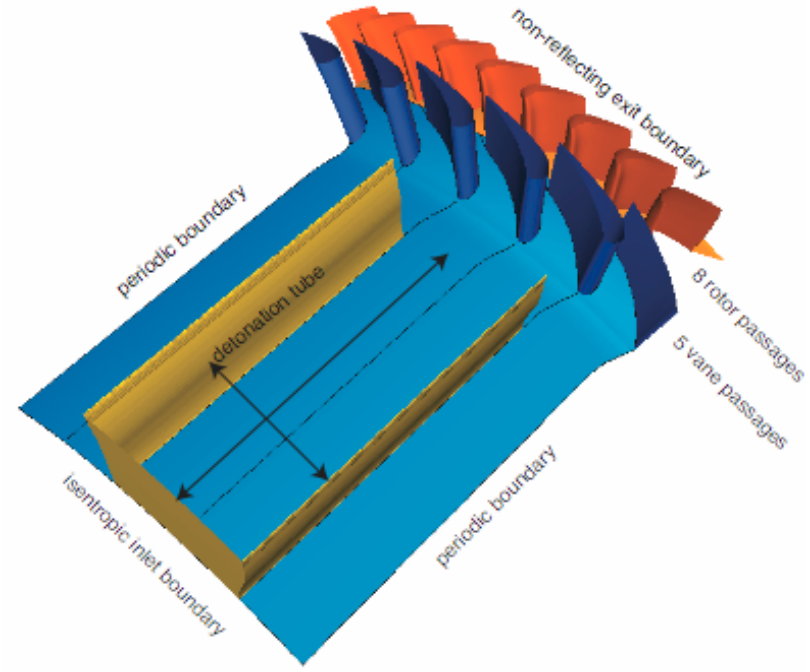

Figure 1.—The turbine stage geometry with the detonation tube volume embedded in the inlet region of the vane meshes.

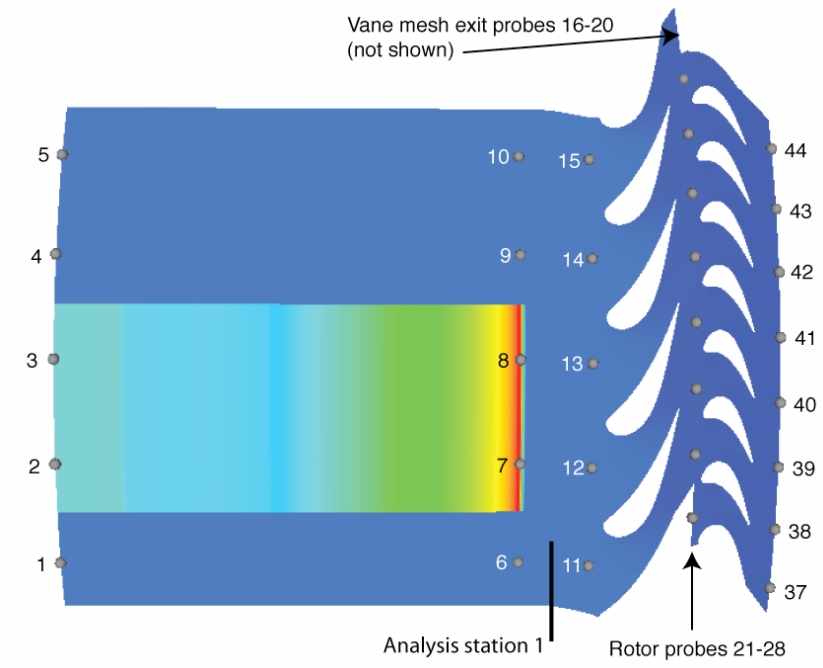

Figure 2.—Static pressure at the initial condition on a midspan surface. Gray dots show numerical pressure probe locations (for clarity, the vane domain exit pressure probes are not shown).

Boundary conditions for the simulation are as follows. The inlet boundary was low-Mach number, isentropic where a radial profile of total pressure, total temperature, and flow angle are specified. The properties are uniform in the tangential direction. Note that this is a reflective type of boundary condition. The exit boundary was two-dimensional non-reflecting with the base flow provided from a steady state simulation of the turbine. The detonation tube was 'constructed' of slip wall boundary conditions on mesh surfaces as illustrated in figure 1. Slip conditions were chosen because the uniform tangential grid spacing was optimum for preserving propagating waves but not adequate to resolve a boundary layer. Both the vane and rotor have cooling flows included by using source terms. The source terms are steady state and will not respond to passage of the shock wave nor will they respond if the turbine is off condition. Numerical pressure probes are also included at seven axial locations at hub, midspan, and casing radial locations. Pressure values are recorded at the axial locations of the inlet, tube exit, vane leading edge, vane mesh exit, rotor mesh inlet, and rotor mesh exit. The pressure probes in the rotor rotate with the blade.

As stated earlier, the detonation tube was modeled as an initial value problem within a volume of cells which were part of the vane meshes. The one-dimensional gas dynamic code of Paxson (ref. 14) was used to calculate the properties in a detonation tube at the instant that the detonation wave was at the tube exit. At the beginning of a tube firing cycle, the conditions from Paxson's code were imposed on the volume of cells comprising the detonation tube in the 3D mesh. See figure 2 for an illustration of the initial condition. The peak pressure and temperature of the detonation was set to 8x the tube reference values based on peak pressure amplitudes measured in detonation tubes operating with hydrocarbon fuels. The calculation was started and the detonation wave propagated from the tube exit and into the turbine domain. This procedure is equivalent to a shock tube calculation. Note that TURBO is not calculating any chemical kinetics (combustion); this was strictly a gas dynamic calculation.

For a fair comparison of turbine performance and for the turbine to operate on design the equivalent conditions at the vane inlet must be the same in the PDC case as in the conventional combustor configuration. The proper definition of the equivalent condition is still uncertain for flows generated by the PDC where large excursions of properties in time and spatial non-uniformities exist. Additionally, the mixing loss experienced by such an unsteady flow is not known a priori. Given these uncertainties, the configuration of the detonation tube for the simulation was based on the following restrictions and assumptions. The goal is to size the detonation tube correctly so that the proper enthalpy is added to the flow and the turbine operates at its design point. The turbine inlet condition is controlled by:

1. The tube firing frequency
2. The choice of inlet total pressure and total temperature
3. The detonation tube exit area

For convenience, the tube firing frequency was assumed to be 86.925 Hz which is ½ the turbine rotational frequency. Therefore, one tube firing/purge cycle required two turbine rotor revolutions. This firing frequency is higher than what has

been demonstrated in detonation tubes with liquid fuels and is, therefore, optimistic. For reference, the turbine first blade passing frequency is 11.126 kHz which illustrates the vastly different time scales present in the problem.

The choice of inlet total pressure and temperature must be based on the anticipated performance of the PDC. As a starting point, the inlet total temperature was set to the compressor exit, T3. The choice of inlet total pressure was more difficult because of two competing requirements. Firstly, assuming limited computing resources, it was desired to have the turbine operating nearly on design for the first detonation tube firing. This required that total pressure be adjusted to match corrected flow based on T3 so that flow angles and loading are correct. For a single tube firing the turbine aerodynamics would be more representative for calculating attenuation. Secondly, if multiple tube firing cycles could be calculated, the turbine inlet conditions would reach some repeatable state where the PDC is (possibly) generating a pressure rise. In this case the inlet Pt should be adjusted to account for the pressure rise and maintain some equivalent turbine inlet pressure, P4. The final value of inlet total pressure was a compromise. The ratio of P4 to inlet Pt was 1.63 which is slightly higher than what maintains corrected flow at T3 and (probably) too low for the PDC to make up in its pressure rise. Ideally, the PDC pressure ratio would be determined from a simulation and the inlet pressure adjusted. Within resource constraints, this was not done for this work and the turbine will be somewhat off design.

The third independent variable is tube area. It is not physically possible to generate a detonation in tubes that are too small or too large in diameter. Many hybrid engine conceptual designs also have bypass flow around the tubes for cooling purposes. In other words, a small, narrow tube is not a good choice and a tube that is the whole annulus is also not realistic. Some initial 2D calculations indicated that a tube the width of a single vane passage is not large enough to add sufficient enthalpy. A tube the width of two vane passages appeared adequate and was used for the 3D simulations.

Tube purge was implemented by changing the boundary condition on the head end of the tube from slip wall to isentropic inlet. The fraction of cycle at which purge begins is, of course, configuration dependent. Purge timings are shown in the next section.

Simulation Convergence

A small time step is necessary to maintain code stability. A 1D version of the numerical algorithm implemented in TURBO was used for a shock tube problem in order to help estimate the maximum time step permissible for the turbine calculation. Results from the 1D code indicated that the detonation wave cannot advance more than one node in a time step or numerical instabilities occur. Based on those results a very conservative (small) time step of 1600 iterations per blade passing was chosen for the turbine calculation. This time step is 10 times smaller than what would be used for a typical aerodynamic calculation of a turbine.

Three complete tube firing cycles were calculated. Figure 3 shows the static pressure trace from the Probe 12 location at mid-span. Probe 12 is located at the vane inlet plane directly downstream of the detonation tube as shown in figure 2. The start of the tube purge cycles are shown as red lines in figure 3. The boundary condition on the head end of the tube

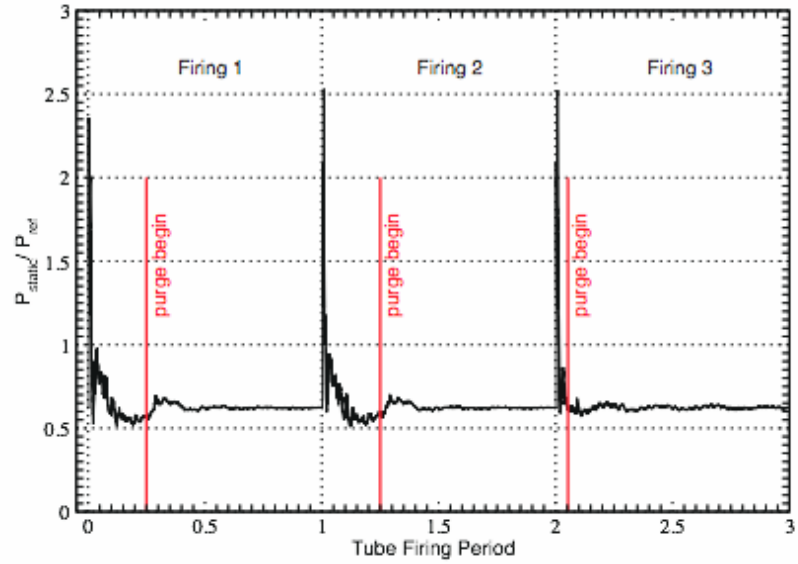

Figure 3.—Static pressure history at the Probe 12 location, mid span showing the three tube firing cycles calculated. Note that the tube purge was started earlier in the 3rd firing cycle to prevent the underpressure that occurred in the previous cycles.

was changed from solid wall to isentropic inlet instantaneously to purge the tube. For the 3rd firing cycle the tube purge was started earlier to prevent the underpressure from occurring. The pressure traces are now analyzed in more detail.

Pressure Transmission Loss Through the Turbine Stage

In this section the static pressure transmission loss (PTL) through the turbine stage is computed using the simulation data. While pressure histories have been obtained at hub, mid-span and casing locations for some 36 "probe" locations in the computational domain (see fig. 2), the main interest in this section is to determine the average PTL through the turbine stage. As such, only the probes immediately upstream of the vane (i.e., 11 through 15), those between the vane and the rotor (i.e., 16 through 28), and those downstream of the rotor (i.e., 37 through 44) are relevant. Furthermore, since we seek to find the average pressure transmission loss through the stage, the fine details of pressure time histories at the various probe locations are ignored. In any case, the basic waveforms (and hence, their spectral content) are similar save for amplitude differences and some fine scale details in each axial plane making the averaging of the spectra a reasonable assumption. For example, in figure 4, computed pressure histories for locations just upstream of the vane are plotted. In the left frame of this figure, the time histories corresponding to the hub, mid-span and casing stations are plotted for the probe location 13. Except for the amplitude differences, the basic waveforms are quite similar. The same is true when comparing the waveforms for the five mid-span probes just upstream of the vane, namely 11 through 15. Therefore, in what follows the spectra are shown in an average sense. The averaging is done in two stages. First, the spectra for hub, mid-span and casing stations are averaged for each probe location. Then, the average spectra for three regions are computed. These are region 1 just upstream of the vane, region 2 between the vane and the rotor, and region 3 just downstream of the rotor.

It should be noted that the pressure time histories at probes 11 through 20 were extracted from the computational blocks in the stationary frame of reference, while those at probes 21 through 44 were extracted from the computational blocks in the rotating frame of reference. While the magnitude of static pressure is independent of the frame of reference, its frequency content is dependent on the frame of reference. Therefore, the spectra for the "stationary" probes show harmonic content at the so-called blade-passing-frequency (i.e., multiples of 11.126 kHz) and the spectra for the "rotating" probes show harmonic content at the vane-passing-frequency (i.e., multiples of 6.965 kHz).

This is clearly evident in time-frequency plots shown in figure 5. These show spectrally averaged data across the span at four probe locations. The top left frame shows the results for probe 13, the top right frame for probe 18, the bottom left frame for probe 25, and the bottom right frame for probe 44. The blade-passing-frequency harmonics for the stationary probe 18, and the vane-passing-frequency harmonics for the rotating probes 25 and 41 are clearly evident as vertical streaks. Note that there is little evidence of the blade-passing-frequency content upstream of the vane. This is likely a consequence of the high speed flow through the vane passages impeding the upstream propagation of waves. It is also interesting to note the evolution of the spectral content as a function of time. Within each detonation pulse period (around 11.3 msec), as time is advanced (i.e., vertical scale) the initially rich spectral content of the detonation wave gives way to dominantly harmonic content (driven by the blade row interaction) until the next pulse is introduced. It should be noted here that while the spectral information exist up to the Nyquist limit of one half of the sampling rate (~8.5 MHz), frequencies relevant to practical application are limited to 50 kHz or less. However, in order to establish trends, spectra are shown to 100 kHz.

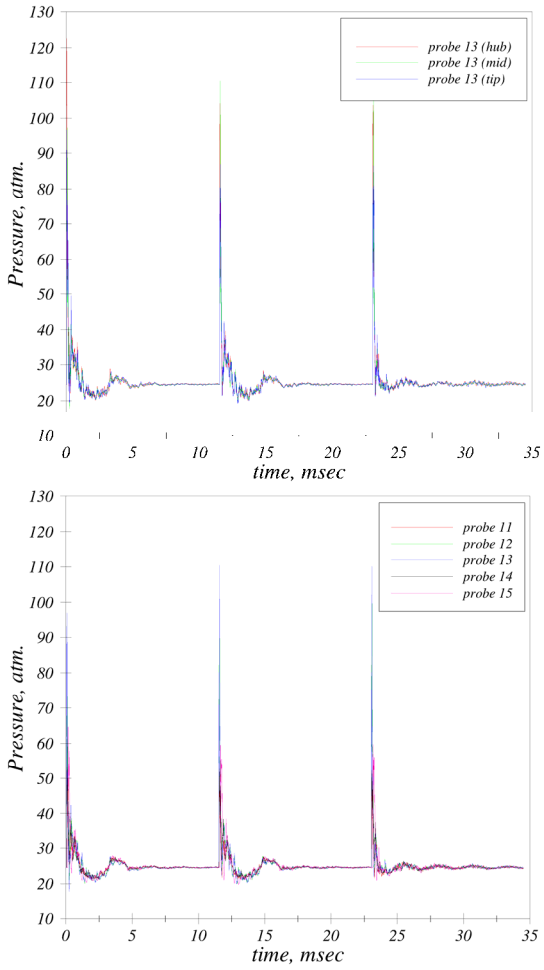

Figure 4.—Pressure time series data from the simulation shown for select points. The left frame shows the time histories for the probe 13 at hub, mid-span and tip locations. The right frame shows the time histories for the mid-span location for probes 11 through 15 all of which are located just upstream of the vane.

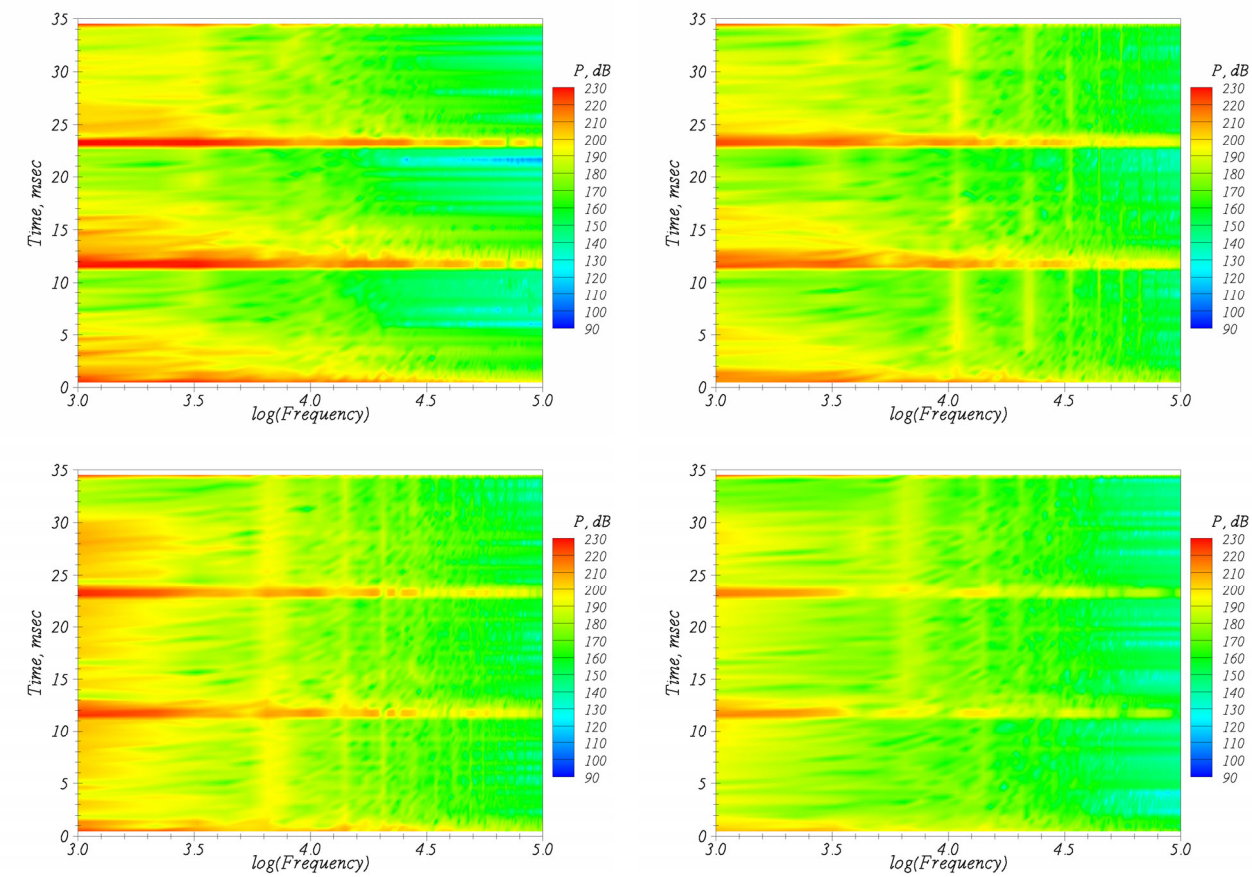

Figure 5.—Time evolution of the frequency content of the unsteady pressure in the vicinity of the turbine stage at four locations. Top left frame is for a point just upstream of the vane, top right and bottom left frames are for points between the vane and the rotor, and the bottom right frame for a point downstream of the rotor. The top frames show simulation pressure histories sampled using stationary "probes" and the bottom frames show simulation pressure histories sampled using rotating "probes". Note the preponderance of vertical streaks in the top right and two bottom frames. The ones in the top right frame represent the blade-passing-frequency harmonics (multiples of 11.126 kHz), and the ones in the bottom frames represent vane-passing-frequency harmonics (multiples of 6.965 kHz).

In figure 6, the probe-wise average spectra in each region are further averaged in groups in order to obtain representative spectral pressure levels ahead of the vane, between the vane and the rotor, and downstream of the rotor. These averaged spectra are represented by the red curve in region 1 (the average of the data from probes 11 through 15), the orange curve in region 2 (the average of the data from probes 16 through 20), the black curve in region 2 (the average of the data from probes 21 through 28), and finally the gray curve in region 3 (the average of the data from probes 37 through 44). Note that the red and orange curves are spectra from stationary probes, and the black and gray curves spectra from the rotating probes. The blade-passing-frequency and vane-passing-frequency content are clearly evident in these representative regional spectra too.

The final step is to compute the blade row PTLs by subtracting the matched sets of the spectra upstream and downstream of each blade row. The stage PTL is then formed by adding the individual blade row PTLs. The results are shown in figure 7. The red curve is the transmission loss across the vane, the black curve the transmission loss across the rotor, and the blue curve a straightforward sum of the two representing a good approximation to the transmission loss across the stage. It should be noted that summing the individual blade row PTLs is legitimate in the average sense, since we are not interested in fine-detail frequency-by-frequency transmission loss information in which case it would be necessary to appropriately interpret the frequency content in the rotating frame in order to do a legitimate frequency-by-frequency subtraction of the spectra upstream and downstream of the stage thus circumventing the need for the intermediate interstage information. Therefore, accepting this approximation, the average pressure transmission loss across the stage is estimated to be ~15 dB (note the light blue curve fit through the stage PTL). This is substantially more than the simple transmission loss estimate obtained in an internal NASA study a few years ago, which determined the turbine transmission loss to be ~5 dB per stage (ref. 2).

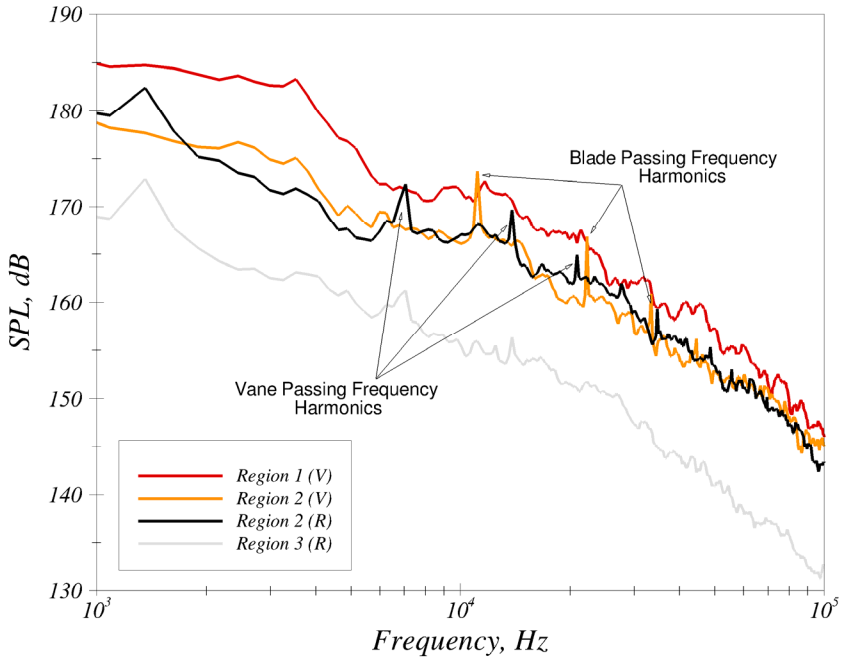

Figure 6.—Region-averaged spectra for points upstream of the vane (red curve), between the vane and rotor (orange and black curves), and downstream of the rotor (gray). The red and orange curves are derived from simulation data obtained from stationary "probes" and the black and gray curves are derived from simulation data from rotating "probes". Note the blade- and vane-passing-frequency harmonic content.

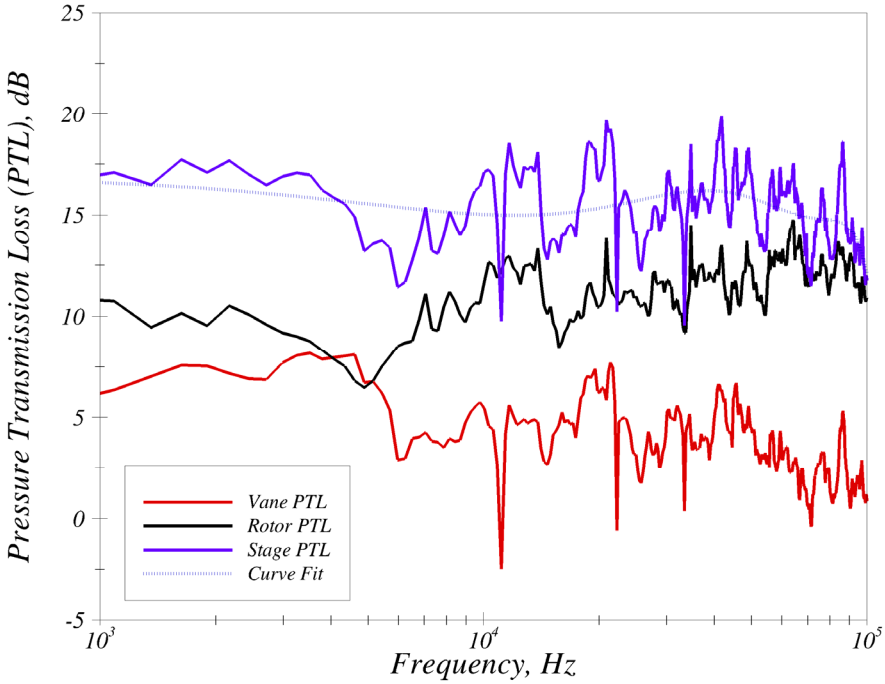

Figure 7.—Pressure transmission loss (PTL) as a function of frequency. Red curve is the PTL across the vane, black curve is the PTL across the rotor, and blue curve is the combined (spectral sum) of the two representing the PTL across the stage. The light blue line through the stage PTL plot is a curve fit to provide estimates of the PTL as a function of the frequency.

It is worth noting that when the individual blade row transmission loss data is examined, it is clear that while both blade rows are effective in attenuating the low-frequency content, the rotor is significantly more effective in mitigating the high-frequency content than is the vane. This is partially due to the higher count (smaller pitch) for the rotor compared with the stator, but there are likely additional justifications too which are not explored in this paper.

Turbine Aerodynamic Performance

Determining the efficiency of a cooled turbine is difficult due to the need to define the ideal work output with contributions from the cooling flows (ref. 15). There is no industry standard method. With the current simulation there was the added complexity of the impulsive inflow to the turbine. The analysis began by looking at the time history of some averaged quantities that would typically be used to determine turbine performance.

To do the averaging, three analysis stations were defined: tube exit, interface, and rotor exit. The tube exit station was slightly downstream of the actual tube exit but is in a region of where the mesh lines were at constant axial locations. See figure 2. The interface station was midway between the vane trailing edge and the rotor leading edge. The rotor exit station was one cell upstream of the rotor mesh exit plane. Both the interface and rotor exit stations were on mesh faces where the mesh lines had constant axial positions.

The averaging was done over the above mesh planes within the 3D flow fields. As such, it was impractical to store the 3D flow field for every time step. 3D solutions were stored at a frequency of 10 per rotor blade passing period for the first 2.2 msec and 2 per rotor passing period for the remainder of the firing cycle. This gave 241 averages during the most active part of the firing cycle and 209 averages during the tube purge portion of the cycle where the conditions were quasi steady. The analysis was done using the linear variable specific heat model described by Turner (ref. 16).

The first quantity analyzed is mass flow. Figure 8 shows dimensionless mass flow at the three analysis stations versus time. The initial portion of the firing cycle is shown in more detail in the lower plot. The detonation tube firing is characterized by a strong jet of mass flow as shown by the peak in the tube exit curve. The vane passages directly downstream of the tube cannot accommodate the mass flow rate. This causes a back flow and circumferential spreading of the hot gasses as seen in figure 9 and as indicated by the negative mass flow from the tube exit station in Fig. 8. Eventually the vane passages can accommodate the flow exiting the tube and the back flow ceases. Note also the mass addition due to the vane and rotor cooling flows is apparent by the offset of the three curves during the purge portion of the cycle. The cooling flows are a significant portion of the throughflow and must be accounted for in any performance calculations. The presence of reverse flow at the tube exit station makes the use of the typical mass weighted average quantities problematic.

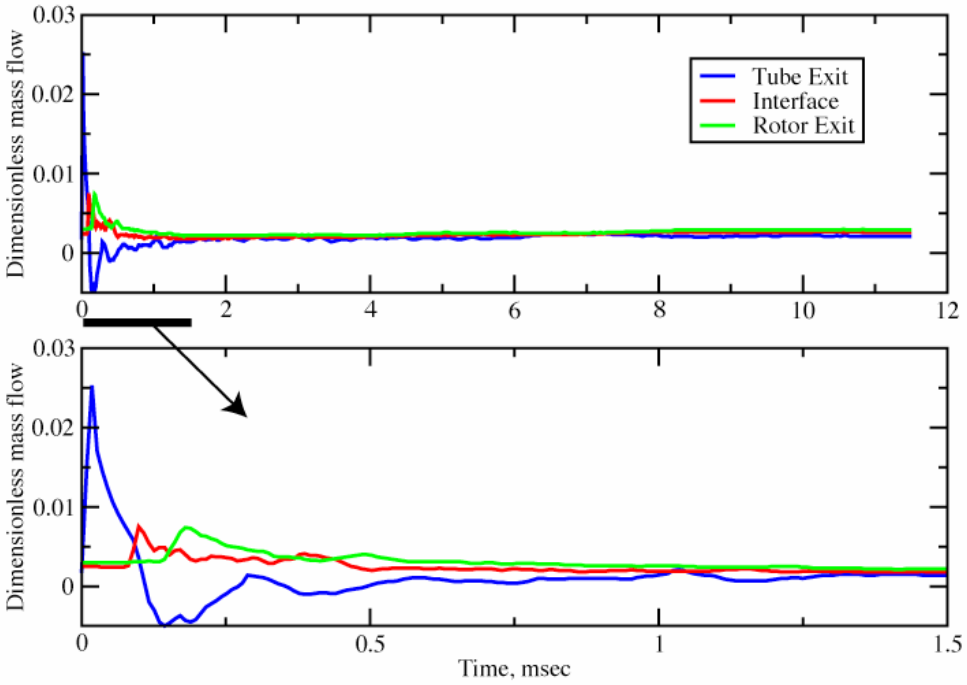

Figure 8.—Dimensionless mass flow at the three performance analysis stations. The upper plot shows the entire Firing 3 time history. The lower plot is a detailed view of the first 1.5 msec of Firing 3. The tube purge begins at 0.6 msec.

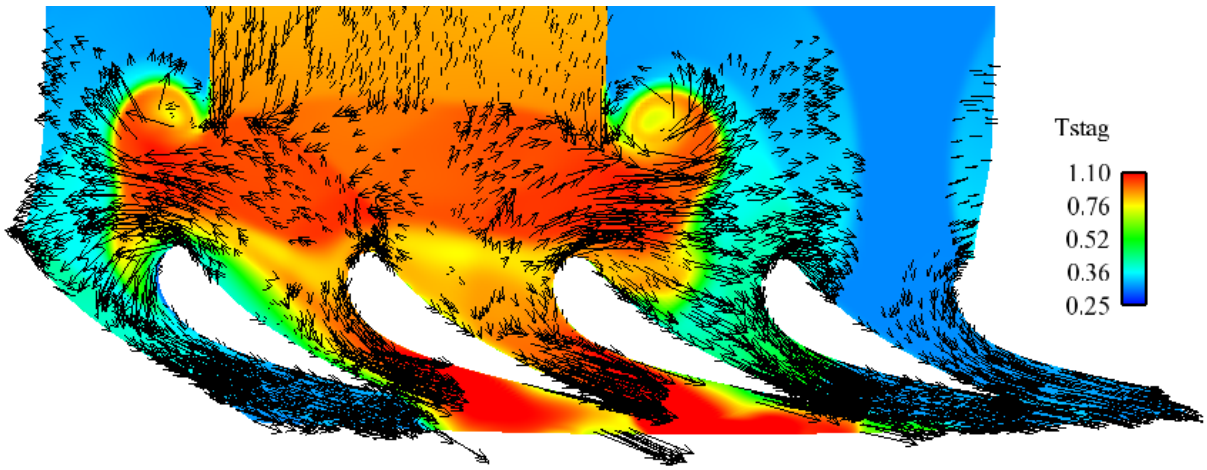

Figure 9.—Instantaneous view of reverse flow at the inlet of the vane passages directly downstream of the detonation tube. This reverse flow appears as a negative mass flow for the tube exit station shown in figure 8.

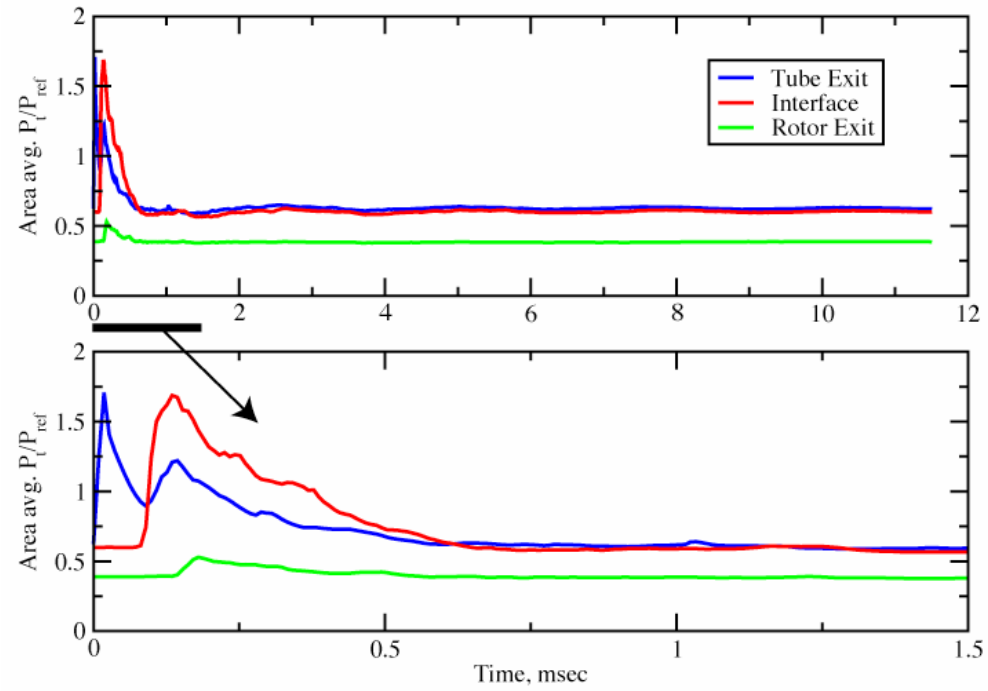

Figure 10.—Area average total pressure at the three performance analysis stations.

Figure 10 shows the area average total pressure, Pt, versus time for the complete cycle and a detail of the initial detonation wave passing. Area weighting is used for illustrative purposes because the typical mass weighted average is ill defined for reverse flow. The total pressure behaves as expected through the turbine. Note that these are area averages and the peak pressure amplitude can be much greater for an individual region of the flow. Figure 11 shows the focusing of the detonation wave by the pressure surface of the vane. Very high static pressure is present (~100 atm) albeit for a very brief time period.

Figure 12 shows the total enthalpy flux versus time. The backflow at the tube exit shows as a negative flux of enthalpy.

Based on the mass weighted averages, the curves are integrated in time to yield a 1D performance number for Firing cycle 3. First the performance of the pulse detonation combustor is given in table 1. The pressure and temperature ratio are based on the mass weighted average tube exit Pt and Tt divided by the inlet conditions. The PDC performance is compared to a conventional combustor. The PDC does produce a pressure rise as intended but falls short of reaching the pressure ratio necessary (1.60) to achieve the turbine

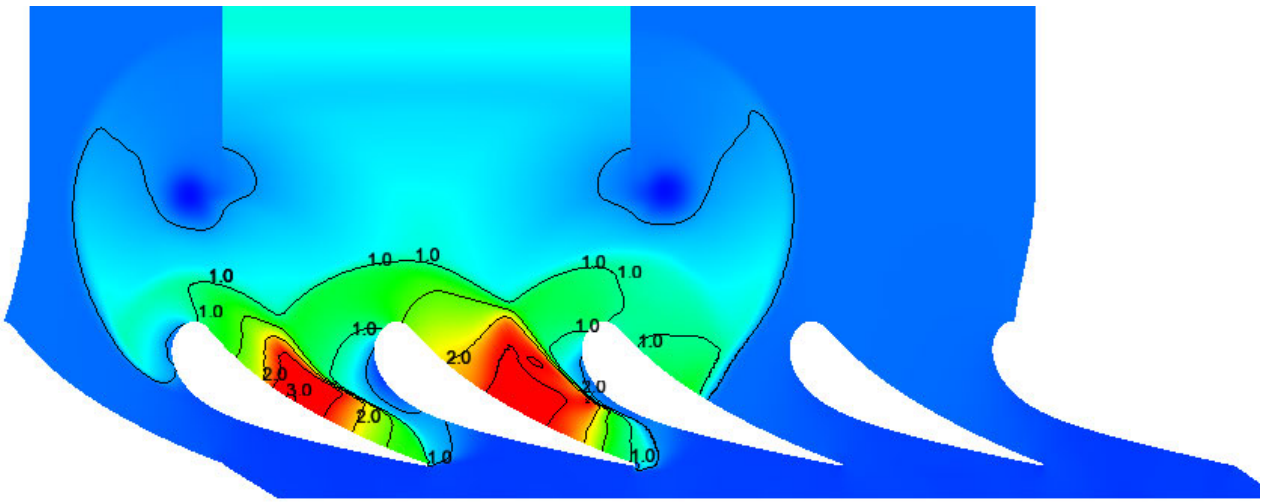

Figure 11.—Instantaneous view of the focusing of the detonation wave by the concave curvature of the vane pressure surface. Normalized static pressure is shown. Peak pressure is ~3x reference pressure.

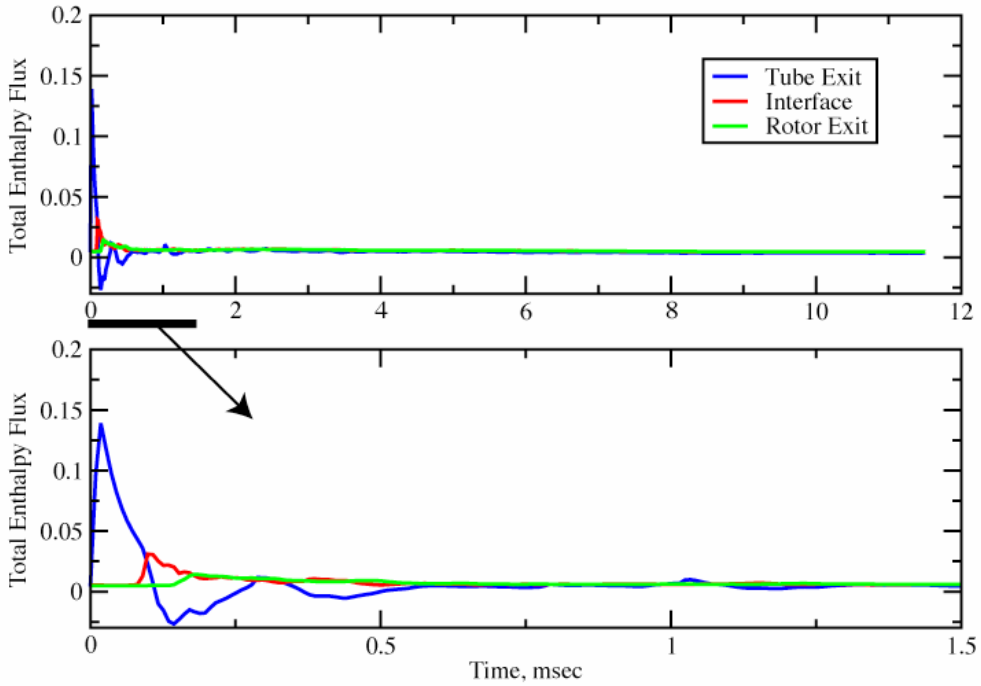

Figure 12.—Flux of total enthalpy at the three analysis stations. The upper plot shows the entire Firing 3 cycle. The lower plot shows a detailed view of the first 1.5 msec of Firing 3.

design condition inlet Pt. The enthalpy introduced is also not adequate to reach the design Tt. As stated in the introduction, this outcome was surmised at the outset of the calculation but the exact performance of the PDC could not be known a priori. It is now evident that the enthalpy input must be increased by 50% to reach the turbine design condition. This could be done by increasing the tube area by 50% or by increasing the tube firing frequency.

TABLE 1.—PULSE DETONATION COMBUSTOR PERFORMANCE COMPARISON.

	PDC	Conventional
Pressure ratio	1.09	0.95
Temp. ratio	1.33	2.10

The performance across the turbine stage is given in table 2. As stated earlier, the calculation of the performance was not straightforward and the analysis was as follows.

TABLE 2.—TURBINE STAGE AERO PERFORMANCE WITH PDC INFLOW.

Pressure ratio Inlet to exit	Enthalpy ratio Inlet to exit	Efficiency
1.72	1.17	~26.7%

The possible advantage of an impulsive inflow is the ability to extract more work through unsteady processes. For example, in a conventional steady flow turbine the typical inlet radial profile of total temperature will always cause a loss due to mixing because the steady flow has no method to recover the inherent availability in a temperature gradient. In an unsteady process there is the possibility of 'moving' energy from one form to another that is capable of producing useful work. The moving shock wave produces a static pressure rise but much of its energy is dissipated as heat. However, when the shock interacts with the turbine (the shock focusing of fig. 11) more of the energy may be converted to static pressure from which useful work can be extracted by the turbine.

The H-s diagram of figure 13 indicates that unsteady processes may be important. The solid curves represent constant Pt lines based on the integrated mass-weighted average Pt at the three analysis stations. The symbols are integrated mass-weighted normalized enthalpy and entropy plotted directly. For a steady process the symbols would lie directly on the curves. The symbols being above the curves indicates that more energy is potentially available to do work than what was expected. Further investigation is necessary to fully explain this result.

To determine the turbine efficiency the actual work and ideal work must be calculated including the influence of cooling flows. Figure 14 shows the H-s diagram for the efficiency calculation. To determine the turbine stage exit condition a constant Pt line based on the integrated H and s was constructed. In other words, the constant Pt curves goes through the integrated exit H-s point (green diamond symbol). For the inlet condition the cooling flows were assumed to enter at the inlet integrated mass-weighted Pt (triangle symbol). The coolant flow fraction is 41.6% of inlet flow. A mixed inlet condition was constructed as the mass weighted average of the coolant and powerstream enthalpies (asterisk symbol). The ideal exit condition is simply the intersection of a constant entropy line with the exit Pt curve. The actual work is the difference in the mixed inlet and integrated exit enthalpy. This ratio gives an efficiency of 26.7%. For comparison, a similar cooled turbine is the E^3 HPT. This *two-stage* turbine had a thermodynamic efficiency of 88.5% at its design condition (refs. 17 and 18). The turbine in the current simulation is off design (inlet flow rate is low because Pt and Tt are lower than design) and the coolant flow fraction is too high (the E3 turbine had 15% cooling flow relative to the inlet flow). A true and fair comparison is difficult at this time. More work is necessary to understand all of the mechanisms at work and to reach a definitive answer for turbine efficiency given an impulsive inlet flow.

Conclusions

A detonation tube – turbine interaction was simulated using the TURBO solver. The numerical results were analyzed to determine the spectral average pressure transmission loss (PTL) and turbine stage performance.

The turbine stage very effectively attenuated all frequencies. The total attenuation was on the order of 15 dB per stage.

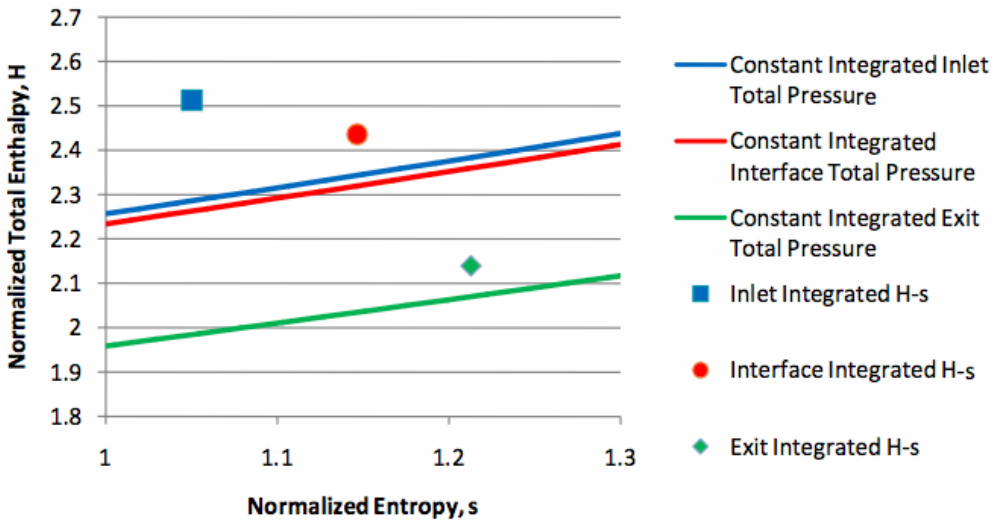

Figure 13.—Enthalpy- entropy diagram for the turbine stage based on integrated quantities.

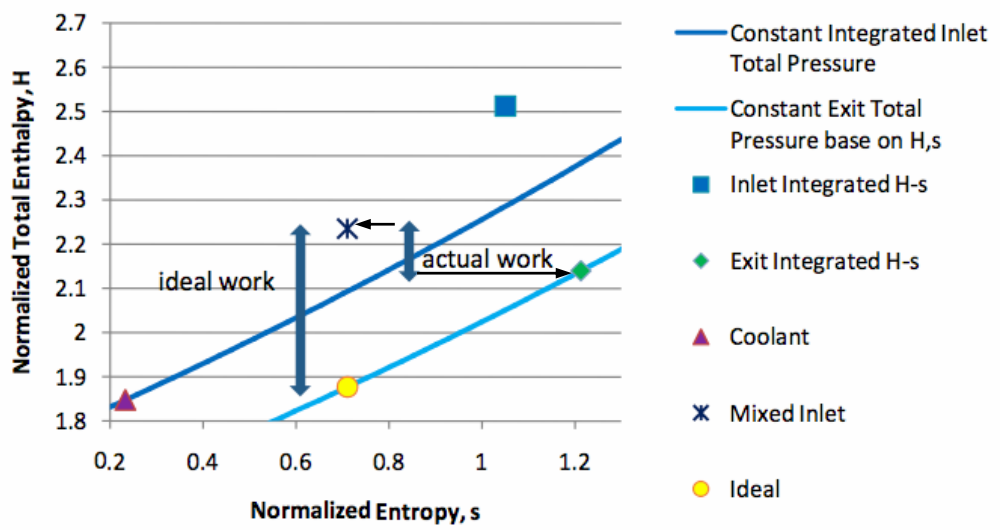

Figure 14.—Enthalpy- entropy diagram showing the stage efficiency definition.

Detailed performance analysis showed some unusual behavior when attempting to use standard steady state turbine performance metrics. The results seem to indicate that unsteady processes play a significant role in the turbine performance. Based on assumptions stated in the paper, a turbine efficiency of 26.7% was determined. Because the turbine was significantly off-design, no definitive conclusion is possible at this time regarding the ability of a conventional turbine to utilize efficiently the impulsive flow from a pulse detonation combustor.

References

1. Schauer, Fred, Bradley, Royce, and Hoke, John, "Interaction of a Pulsed Detonation Engine with a Turbine," AIAA-2003-0891, 41st AIAA Aerospace Sciences Meeting and Exhibit, Reno, NV, Jan. 6-9, 2003.
2. Envia, Edmane, personal communication.
3. Rasheed, Adam, Furman, Anthony, and Dean, Anthony J., "Experimental Investigations of an Axial Turbine Driven by a Multi-tube Pulsed Detonation Combustor System," AIAA-2005-4209, 41st AIAA/ASME/SAE/ASEE Joint Propulsion Conference, Tuscan, AZ, July 10-13, 2005.
4. Caldwell, Nicholas, Glaser, Aaron, Dimicco, Russell, and Gutmark, Ephraim, "Acoustic Measurements of an Integrated Pulse Detonation Engine with Gas Turbine System," AIAA-2005-0413, 43rd Aerospace Sciences Meeting and Exhibit, Reno, NV, Jan. 10-13, 2005.
5. Dean Anthony J., "A Review of PDE Development for Propulsion Applications," AIAA-2007-0985, 45th Aerospace Sciences Meeting and Exhibit, Reno, NV, Jan. 8-11, 2007.
6. Whitfield, D.L., Janus, JM., and Simpson, L.B., 1988, "Implicit Finite Volume High Resolution Wave-Split Scheme for Solving the Unsteady Three-Dimensional Euler and Navier-Stokes Equations on Stationary or Dynamic Grids," MSSU-EIRS-ASE-88-2.20.
7. Roe, P.L., 1981, "Approximate Riemann Solvers, Parameter Vectors, and Difference Schemes," Journal of Computational Physics, vol. 43, pp. 357-372.
8. Osher, S., and Chakravarthy, S. R., 1984, "Very High Order Accurate TVD Schemes," ICASE Report no. 84-44.
9. Steger, J.L., and Warming, R.F., 1981, "Flux Vector Splitting of the Inviscid Gasdynamic Equations with Application to Finite-Difference Methods," Journal of Computational Physics, vol. 40, pp.263-293.
10. Zhu J. and Shih, T.-H., "CMOTT Turbulence Module for NPARC," NASA CR 204143, Aug. 1997."Blade Row Interaction Effects on Compressor
11. Chen, J.P., and Briley W.R., "A Parallel Flow Solver for Unsteady Multiple Bladerow Turbomachinery Simulations," ASME-2001-GT-0348. June 2001, New Orleans, LA.
12. Remotigue, M.G., "Structured Grid Technology to Enable Flow Simulation in an Integrated System Environment," PhD Dissertation, Mississippi State University, Dec. 1999.
13. List, Michael G., Mark G. Turner, JenPing Chen, Michael G. Remotigue, and Joseph Veres, "Unsteady, Cooled Turbine Simulation Using a PC-Linux Analysis System," AIAA 2004-0370, Reno, NV, Jan. 2004.
14. Paxson, D.E., "Performance Evaluation Method for Ideal Airbreathing Pulse Detonation Engines," Journal of Propulsion and Power, vol. 20, no. 5, Sep.-Oct. 2004, pp. 945-947.
15. Young, J.B. and Horlock, J.H., "Defining The Efficiency Of A Cooled Turbine," J. of Turbomachinery, vol. 128, pp. 658-667, Oct. 2006.
16. Turner, M.G., "Multistage Turbine Simulations With Vortex-Blade Interaction," J. of Turbomachinery, vol. 118, pp. 643-653, Oct. 1996.
17. Reed, John A. and Turner, Mark G., "An Entropy Loss Approach For A Meanline Bladerow Model With Coupling To Test Data And 3D CFD Results," GT2005-68608, presented at ASME Turbo Expo 2005, June 6-9, 2005, Reno-Tahoe, NV.
18. Timko, L.P., "Energy Efficient Engine High Pressure Turbine Component Test Report," NASA CR-168289, 1984.

REPORT DOCUMENTATION PAGE	Form Approved OMB No. 0704-0188

1. REPORT DATE *(DD-MM-YYYY)*	2. REPORT TYPE	3. DATES COVERED *(From - To)*
01-09-2007	Technical Memorandum	

4. TITLE AND SUBTITLE
The Attenuation of a Detonation Wave by an Aircraft Engine Axial Turbine Stage

5a. CONTRACT NUMBER

5b. GRANT NUMBER

5c. PROGRAM ELEMENT NUMBER

6. AUTHOR(S)
Van Zante, Dale; Envia, Edmane; Turner, Mark, G.

5d. PROJECT NUMBER

5e. TASK NUMBER

5f. WORK UNIT NUMBER
WBS 561581.02.08.03.03.01

7. PERFORMING ORGANIZATION NAME(S) AND ADDRESS(ES)
National Aeronautics and Space Administration
John H. Glenn Research Center at Lewis Field
Cleveland, Ohio 44135-3191

8. PERFORMING ORGANIZATION REPORT NUMBER
E-16138

9. SPONSORING/MONITORING AGENCY NAME(S) AND ADDRESS(ES)
National Aeronautics and Space Administration
Washington, DC 20546-0001

10. SPONSORING/MONITORS ACRONYM(S)
NASA

11. SPONSORING/MONITORING REPORT NUMBER
NASA/TM-2007-214972

12. DISTRIBUTION/AVAILABILITY STATEMENT
Unclassified-Unlimited
Subject Category: 71
Available electronically at http://gltrs.grc.nasa.gov
This publication is available from the NASA Center for AeroSpace Information, 301-621-0390

13. SUPPLEMENTARY NOTES

14. ABSTRACT
A Constant Volume Combustion Cycle Engine concept consisting of a Pulse Detonation Combustor (PDC) followed by a conventional axial turbine was simulated numerically to determine the attenuation and reflection of a notional PDC pulse by the turbine. The multi-stage, time-accurate, turbomachinery solver TURBO was used to perform the calculation. The solution domain consisted of one notional detonation tube coupled to 5 vane passages and 8 rotor passages representing 1/8th of the annulus. The detonation tube was implemented as an initial value problem with the thermodynamic state of the tube contents, when the detonation wave is about to exit, provided by a 1D code. Pressure time history data from the numerical simulation was compared to experimental data from a similar configuration to verify that the simulation is giving reasonable results. Analysis of the pressure data showed a spectrally averaged attenuation of about 15 dB across the turbine stage. An evaluation of turbine performance is also presented.

15. SUBJECT TERMS
Pulse detonation engines; Axial turbines; Hybrid propulsion

16. SECURITY CLASSIFICATION OF:			17. LIMITATION OF ABSTRACT	18. NUMBER OF PAGES	19a. NAME OF RESPONSIBLE PERSON
a. REPORT	b. ABSTRACT	c. THIS PAGE			STI Help Desk (email:help@sti.nasa.gov)
U	U	U	UU	18	19b. TELEPHONE NUMBER *(include area code)* 301-621-0390